Multi Physics Model of a Nickel Based Battery Suitable for Hybrid Electric Vehicle Simulation

Loïc Boulon [1], Daniel Hissel [2], and Marie-Cécile Péra [3]

[1] *FEMTO-ST UMR CNRS 6174, University of Franche-Comte, loic.boulon@univ-fcomte.fr*
[2] *FEMTO-ST UMR CNRS 6174, University of Franche-Comte, daniel.hissel@univ-fcomte.fr*
[3] *FEMTO-ST UMR CNRS 6174, University of Franche-Comte, marie-cecile.pera@univ-fcomte.fr*

Abstract

This paper deals with the modelling of a nickel-based battery. The objective is to design a model usable in an electrical engineering laboratory. This study provides a State of Charge (SoC), current and temperature dependant experience-based model. The parameterization is really fast and simple; it does not require electrochemical knowledge. In this paper, the parameterization tests and their analyses are detailed. This model is experimentally validated.

Keywords

battery, nickel, temperature, experimental based model

1. INTRODUCTION

Considering environmental protection issue, the development of Hybrid Electric Vehicles (HEV) is a major important preoccupation. Today, the battery performances allow their integration in such a vehicle [Chan, 2007]. Nevertheless, the research and development costs are very high and the virtual prototyping is a mandatory step to reduce them. One of the difficulties of the HEV modelling is to work in many physical fields. Actually, an overall HEV model has to take into account the interactions between electrical, mechanical, thermodynamic or electrochemical parts. Usually, this work is realized in electrical engineering laboratories. However, the researchers are not specialized in every required physical field and don't have each experimental equipment at one's disposal.

This paper deals with the modelling of the voltage behaviour of a battery [Boulon et al., 2008]. The objective is to propose a model that doesn't require electrochemical knowledge or specific scientific devices. The model developed in this study can be simply used and parameterized in an electrical engineering laboratory. The literature already proposes many battery models. However, it is quite difficult to find a good compromise between the model complexity and the model accuracy. On the one hand, electrochemical specialists propose very accurate model but they are difficult to apprehend and they involve complex parameterization algorithms [Thele et al. 2008]. Moreover, most of the time, they require costly experimental devices like impedance spectrometers [Nelatury and Singh, 2007]. On the other hand, electrical engineers proposed good models for the old battery technologies like lead-acid batteries [Van Mierlo et al., 2004; Cereaolo, 2000]. However, they are too basic to represent some important phenomena. For example, the nickel batteries present a hysteretic behaviour of the Open Circuit Voltage (OCV).

This work describes a simple multi-physics modelling process, including temperature dependency.

2. MODELLING PRINCIPLES

As explained, the main idea is here to design an experimental protocol to parameterize the battery model. The first step presented in this part is to identify a model structure able to represent the voltage behavior of a single cell.

2.1 Model structure

The chosen model is based on an equilibrium open circuit potential E_0 and an internal resistor $R_{i\,batt}$ (Figure 1) [Eshani et al., 2005]. E_0 is measured at the cell terminals with $I_{cell}=0$ and after stabilization. $R_{i\,batt}$ is defined as (1).

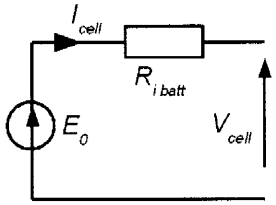

Fig. 1 Electric scheme of the battery model

$$R_{i\_batt} = \frac{E_0 - V_{cell}}{I_{cell}} \quad (1)$$

As a consequence, the model is composed by two parameters. Nevertheless, these parameters are not fixed. These values can be influenced by the solicitations on the batteries like the current, the temperature or the SoC. The effective influence will be studied in the next part.

(1) Current

I_{cell} is the current inside one battery element. Its sign is positive on a discharge phase (source convention).

(2) Temperature

T_{batt} represents the electrolyte temperature (and not the ambient temperature). The temperature results from the environment of the battery but also from the electrical solicitations. Basically, the presence of a current through the internal resistance leads to losses dissipated in form of heat. As a consequence, for a test at a given temperature, the heating of the battery has to be controlled.

(3) SoC

The SoC estimation is a recurrent problem considering electrochemical devices [Verbrugge and Tate, 2004]. Here, the model doesn't aim to provide a very accurate description of the battery. This model will be integrated in a complete power system simulation (for example in an EV or HEV simulation). Each component of the system has then to be represented at the same level of details. As a consequence, the chosen SoC estimator is a simple coulometric counter as given by (2)

$$SoC = SoC_{init} + \frac{100}{C_N}\int I_{cell}\,dt \qquad (2)$$

with C_N (in Ah.) the rated capacity of the battery.

2.2 Experimental tests

All tests are performed on a nickel-cadmium STH 600 Saft battery (C_{cell}=60Ah, V_{cell}=1.3V) [Boulon et al. 2008]. All the tests are performed in a thermal room and the evolution of the electrolyte temperature is controlled.

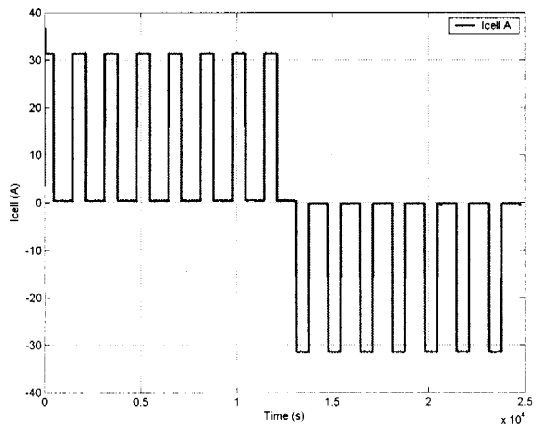

Fig. 2 Current profile of the [30A-20°C] test

This control is performed by a thermocouple located in the liquid electrolyte. The variation is under 2 °C during a cycle and here considered as negligible. The battery cell is charged and discharged with an alternating current profile (Figure 2).

When a current is applied, the SoC changes and V_{cell} can be measured. Without any current, the open-circuit potential E_0 is measured. The OCV measurement has to be performed after stabilization (which occurs after approximately 1000 seconds) [Srinivasan et al. 2001].

The SoC is calculated from the current evolution and the voltage behavior can be plotted versus the SoC (Figure 3). The OCV E_0 and the cell voltage V_{cell} are extracted from this plot. With these two voltages, the internal resistor is calculable. Each experimental result shown in this study is extracted from this plot. This test is carried out for three current levels and three temperatures. The extreme current and temperature tests delimit the validity range of the model.

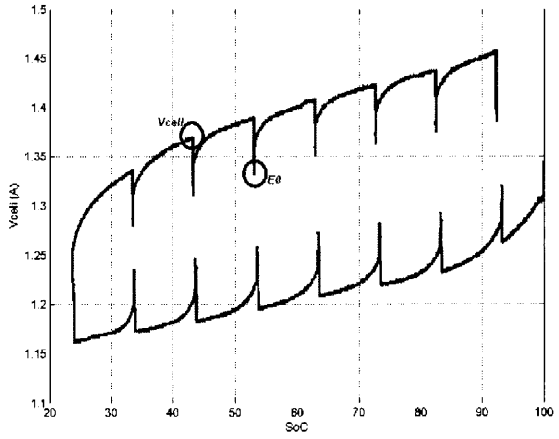

Fig. 3 Evolution of the cell voltage versus the SoC for the [30A-20°C] test

After each test, the battery is fully recharged according to the manufacturer protocol. The I_{cell} current is fixed to 12A (0.2C_5 A) until V_{cell} reaches 1.55V. After that, a current of 3A (0.05C_5 A) is imposed for 4 hours.

3. EXPERIMENTAL RESULTS

3.1 Constant temperature study

Firstly, a constant temperature (20°C) study has been performed. Figures 4 and Figure 5 show respectively the evolution of E_0 and of R_i with a variable SoC. Tests are performed at three different currents in charging and discharging phases.

Figure 4 shows the hysteretic behavior of the open circuit voltage. E_0 is not directly SoC dependant [Thele et al., 2008]. As a consequence, with a nickel based battery, the OCV is hardly usable to design a SoC estimator [Verbrugge and Tate, 2004]. In a discharging phase, the

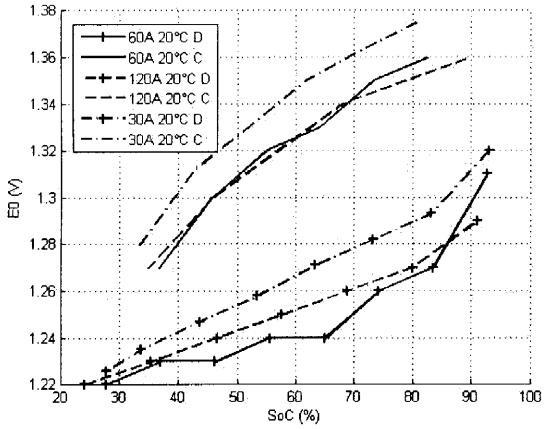

Fig. 4 Evolution of E_0 versus the SoC for different currents (experimental results). C: Charging phase ; D: Discharging phase

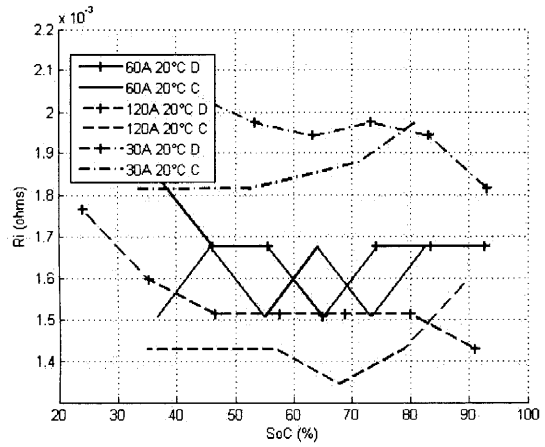

Fig. 5 Evolution of $R_{i\,batt}$ versus the SoC for different currents (experimental results)

OCV follows the lower bound of the shape; and in a charging phase, the OCV follows the upper bound. Moreover, the literature shows other hysteresis inside the first one [Thele et al., 2008]. When the current sign changes, the OCV does not jump between the two sides of the hysteresis. There is a delay in the OCV between the two boundaries.

Figure 5 shows that the SoC is not a significant parameter on the R_i value. Nevertheless, for high SoC R_i is decreasing in discharge phase and is increasing in the charge phase. In this figure, it appears clearly that the R_i parameter is highly current dependent.

3.2 Constant current study

Secondly, the influence of the temperature has been studied. Tests are performed for three different temperatures in charging and discharging phases (I_{cell}=±60A). Figure 6 shows the evolution of E_0, its value is globally higher at 20°C (the rated temperature specified by the manufacturer).

Figure 7 shows the evolution of R_i, its value is decreasing with an increasing temperature. Consequently, the energetic performances of the cell increases with the temperature. It has to be noticed that the influence of the SoC on the internal resistor is more sensitive at low temperature.

The next section presents an empirical modelling of the cell from the previous experimental results.

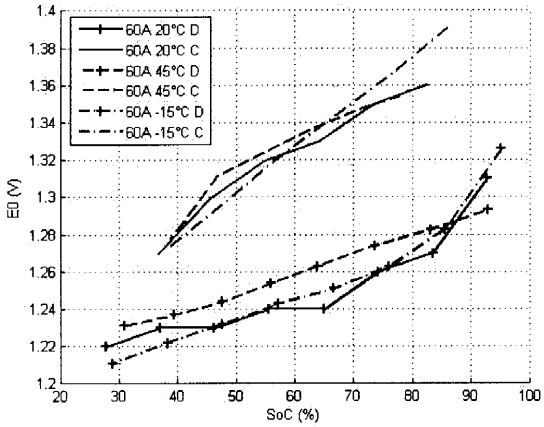

Fig. 6 Evolution of E_0 versus the SoC for different temperatures (experimental results)

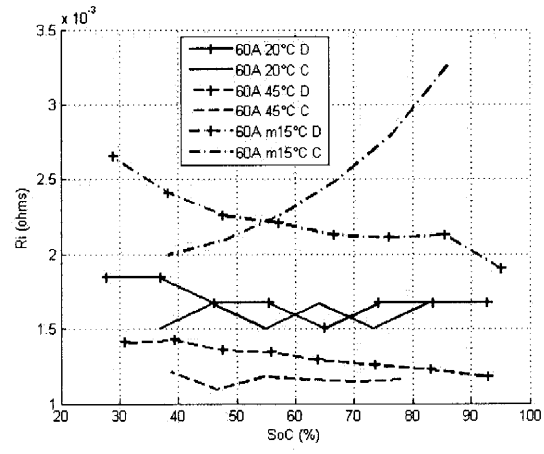

Fig. 7 Evolution of Ri_{batt} versus the SoC for different temperatures (experimental results)

4. MODELING OF THE CELL

In this part, the modelling of the cell will be presented. For each influential factor (the SoC, the temperature and the current), hypothesis and modelling choices will be performed. One more time, the objective is here to provide a simple and fast-to-parameterize model. All the parameters are fitted by a Newtonian optimisation algorithm (for example, available in the Matlab 'fmincon' function).

4.1 Influence of the SoC

The SoC influence on $R_{i\,batt}$ is neglected. Actually, the SoC modifies $R_{i\,batt}$ in extreme conditions (very low temperature). Nevertheless, these conditions are not often reached during real cycles. The influence of the SoC on the OCV is noticeable and the hysteresis must be taken into account. Nevertheless, the transition between the lower and the upper side of the hysteresis is not instantaneous when the sign of the I_{cell} current is changing. In this study, this effect is not represented. To summarize, the SoC dependency of E_0 has been modelled as shown in Figure 8. The two sides of the hysteresis are represented with linear functions (3):

$$E_0 = aSoC + b \tag{3}$$

with a and b taking different values in the charging and the discharging phases.

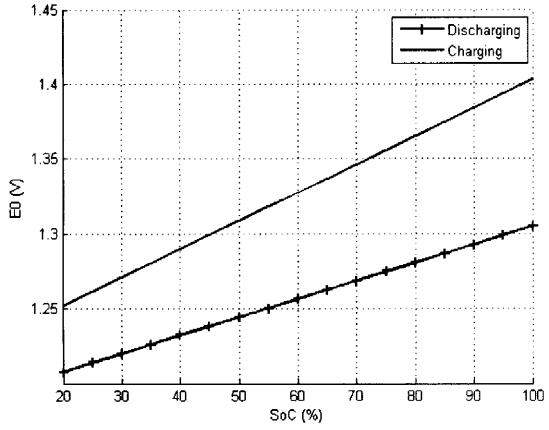

Fig. 8 Evolution of E_0 versus the Soc (model)

4.2 Influence of the current

The influence of I_{cell} on the open circuit potential is neglected. The behavior of the internal resistance is fitted with a second order polynomial function (Figure 9).

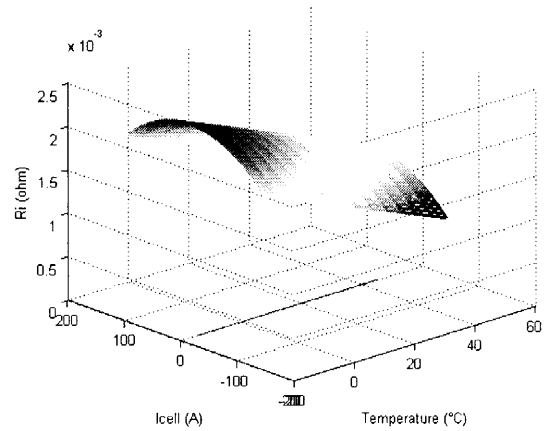

Fig. 9 Evolution of $R_{i\,batt}$ versus the current and the temperature (model)

4.3 Influence of the temperature

Its influence on the open circuit voltage is neglected. The temperature dependence of the internal resistance can be approached with a linear or quadratic model (4).

$$R_i = aTemp^2 + bTemp + c \tag{4}$$

5. MODEL EVALUATION

Figures 10, 11 and 12 show comparisons between the experimental results and the simulation results obtained from the proposed model. Firstly, the battery is discharged with current step between 0 and 60 A. Secondly, the battery is recharged in the same way.

The results obtained from the model are pretty close to the experiments. The dynamics of the system is only represented with the SoC variation. Consequently, the dynamic effects when the current level is changing are not taking into account. The main divergences are obtained when the requested current is null. However, at this time, the battery is not used and the knowledge of a closed estimation of the voltage level is not mandatory.

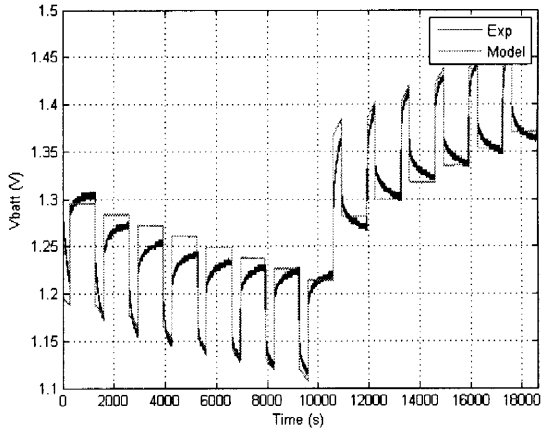

Fig. 10 Comparison between experiment and simulation (Temp=20°C)

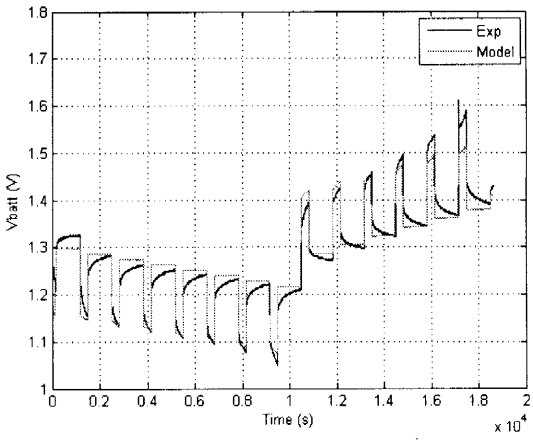

Fig. 11 Comparison between experiment and simulation (Temp=-15°C)

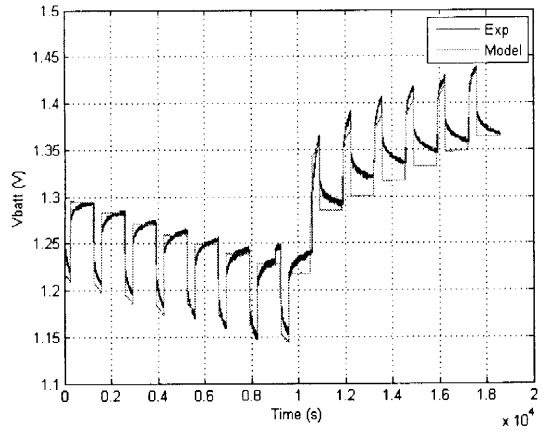

Fig. 12 Comparison between experiment and simulation (Temp=45°C)

These results validate the general approach. With only five easy-to-do experimental tests, the model is parameterized with simple functions (linear or quadratic). Moreover, the hysteretic behavior of the device is managed and the temperature range is really wide.

6. MODELING OF A CELL MODULE

A model of a cell bank [Wong et al., 2006] is obtained by parallel and series coupling of the electric scheme of the model (5, 6).

The modelling of the battery module doesn't take into account any charge balance or aging issues. Moreover, the temperature inside the battery pack is considered as uniform.

$$I_{cell} = \frac{I_{batt}}{n_{cell\_para}} \tag{5}$$

$$V_{cell} = \frac{V_{batt}}{n_{cell\_series}} \tag{6}$$

With V_{batt} and I_{batt}, representing respectively the voltage and the current of the battery module, $n_{cell\ series}$ and $n_{cell\ para}$ are respectively the number of cells with series coupling and parallel coupling in the module.

7. DISCUSSION

As a conclusion, the proposed model does not require electrochemical knowledge. Its parameterization is fast (only 5 experiences) and easy (simple fitting algorithms). Comparison between the experiment and the simulation show the effectiveness of the methodology. The initial objective of a good accuracy – simplicity ratio is achieved in a satisfying way.

Acknowledgements

This work has been made in the MEGEVH-macro national project with the financial support of "Région Franche-Comté", "Region Nord Pas-de-Calais" and Nexter Systems.

References

Boulon, L., D. Hissel, A. Bouscayrol, M-C. Pera, and Ph. Delarue, Multi Physics Modelling and Representation of Power and Energy Sources for Hybrid Electric Vehicles, *Proceedings of VPPC'08*, 2008.

Boulon, L., D. Hissel, and M-C. Pera, Multi-Physics Modelling and Energy Management of a Battery Supercondensator Electric Vehicle Taking Into Account the Operating Temperature Conditions, *Proceedings of Electrimacs'08*, 2008.

Ceraolo, M., New Dynamical Models of Lead-Acid Batteries, *IEEE Transaction on Power Systems*, Vol. 15, No. 4, 1184-1190, 2000.

Chan, C. C., The State of the Art of Electric and Hybrid Vehicles, *Proceedings of IEEE,* Vol. 95, No. 4, 704-718, 2007.

Chan, C. C., S. Liqing, L. Ruchuan, and Q. Wang, Current Status and Future Trends of Energy Storage System for Electric Vehicles, *Journal of Asian Electric Vehicles*, Vol. 6, No. 1, 1055-1060, 2007.

Eshani, M., Y. Gao, S. E. Gay, and A. Emadi, *Modern electric, hybrid electric and fuel cell vehicles*, CRC Press, 2005.

Nelatury, S. R., and P. Singh, Equivalent circuit parameters of nickel/metal hydride batteries from sparse impedance measurements, *Journal of Power Sources*, Vol. 132, No. 1-2, 309-314, 2004.

Srinivasan, V., J. W. Weidner, and J. Newman, Hysteresis during Cycling of Nickel Hydroxide Active Material, *Journal of the Electrochemical Society,* Vol. 148, A969-A980, 2001.

Thele, M., O. Bohlen, D. Uwe Sauer, and E. Karden, Development of a voltage-behavior model for NiMH batteries using an impedance-based modeling concept, *Journal of Power Sources*, Vol. 175, No. 1, 635-643, 2008.

Van Mierlo, J., P. Van den Bossche, G. Maggetto, Models of energy sources for EV and HEV: fuel cells, batteries, ultracapacitors, flywheels and engine-generators, *Journal of Power Sources*, Vol. 128, No. 1, 76-89, 2004.

Verbrugge, M., and E. Tate, Adaptive state of charge algorithm for nickel metal hydride batteries including hysteresis phenomena, *Journal of Power Sources,* Vol. 126, 236-249, 2004.

Wong, Y. S., K. T. Chau, and C. C. Chan, Battery Sizing for Plug-in Hybrid Electric Vehicles, *Journal of Asian Electric Vehicles*, Vol. 4, No. 2, 899-904, 2006.

(Received October 31, 2008; accepted November 4, 2008)